Desalination and Water Treatment
www.deswater.com
doi: 10.1080/19443994.2014.901192

54 (2015) 2601–2610
May

Taylor & Francis
Taylor & Francis Group

Hybrid central composite design optimization for removal of Methylene blue by *Acer* tree leaves: characterization of adsorption

Javad Zolgharnein*, Maryam Bagtash

Faculty of Science, Department of Chemistry, Arak University, Arak 38156-8-8394, Iran, Tel. +98 86 34173400(2042); Fax: +98 86 34173406; email: j-zolgharnein@araku.ac.ir

Received 10 November 2013; Accepted 24 February 2014

ABSTRACT

Statistical experimental design was utilized to optimize the removal of Methylene blue (MB) by *Acer* tree leaves through a batch biosorption process. *Acer* tree leaves were introduced as a novel and low-cost biosorbent for removing MB from aqueous solutions. The influence of various factors, such as initial pH, initial concentration of dye, and sorbent mass on the MB biosorption was investigated. A regression model was derived using a response surface methodology through performing the hybrid central composite design. The proposed quadratic model resulted from the hybrid design approach, which fitted very well to the experimental data. Model adequacy was checked through diagnostic tests, namely analysis of variance; a lack of fit test; and residuals distribution. The optimized condition for MB biosorption was calculated to be pH 2.7; $m = 0.05$ g; and $C = 928$ mg L^{-1}. Furthermore, the isotherms and kinetics of biosorption were also explored.

Keywords: Acer tree leaves; Biosorption; Hybrid composite central design; Methylene blue

1. Introduction

Synthetic dyes are the most serious organic pollutants that are discharged into the environment from textile, plastic, tanning, leather, paints, paper, food processing, and pharmaceutical industries for coloring their products [1]. Methylene blue (MB) is a basic dye, which has been shown to have harmful effects on human being and animals. Inhalation of MB can cause increased heart rate, nausea, and vomiting [2]. Therefore, many methods are available for the removal of dyes from industrial effluents, including photocatalytic degradation [3,4]; sonochemical degradation [5]; micellar-enhanced ultrafiltration [6]; cation-exchange membranes [7]; electrochemical degradation [8]; adsorption/precipitation processes [9]; integrated chemical–biological degradation [10]; integrated iron (III) photoassisted–biological treatment [11]; solar photo-Fenton and biological processes [12]; the Fenton-biological treatment scheme [13]; and adsorption on activated carbon [14,15]. Out of all these methods, adsorption has been found to be superior, since it is an efficient and economical method in the elimination of dyestuffs. Consequently, many kinds of novel adsorbents have been developed and widely applied [2]. The adsorption characteristics of MB on various adsorbents have been extensively investigated [2]. Biosorption as an alternative process offers several advantages, such as low operation cost, minimization of the volume of chemicals, and/or biological sludge to be disposed of, and a high efficiency in detoxifying very dilute effluents. Among biosorbents, the waste

*Corresponding author.

materials and by-products from the agriculture are assumed to be low-cost and effective adsorbents due to their abundance in nature and surface functional groups. Recent studies include the application of agricultural wastes, such as *sugarcane bagasse* [16], *wood shavings* [17], *peanut shell* [18], *peat* [19], *sawdust* [20], *fruit peels* [21], *plant and tree leaves* [22–24], *rice husk* [25], *sugar beet pulp* [26], and *Citrus sinensis bagasse* [27], for the removal of dyes, particularly MB. The ability of biosorbents to remove pollutants is strongly influenced by certain parameters, such as the initial pH, initial concentration of the pollutant, and sorbent mass [24–27]. Therefore, it is necessary to design an appropriate process for maximizing the removal efficiency of pollutants by biosorbents [27,28]. The multivariate optimization has several advantages over the conventional "one-at-a-time" method because it provides more information through running fewer experiments [28–38]. During multivariate optimization, a response surface methodology (RSM) leads to an empirical mathematical model, which relates the removal percent of sorbate with effective variables and their interactions [24,28,31–34]. Among the response surface methods, hybrid design has been less attended by researchers; perhaps due to this it is not well known yet [24,28,29,35]. Hybrid central composite design has more advantages than its regular ones. A lower experimental run, time saving, and a resource-limited situation are its major features [38–40].

The major aim of this study is to demonstrate the potential of *Acer* tree leaves as a new biosorbent for the removal of MB from aqueous waste. It also proposes a proper empirical model that would be able to show clearly, the role of effective variables on MB removal percent. Furthermore, hybrid central composite design is used as a response surface approach to find optimum conditions for maximum MB adsorption capacity uptake (q) from an aqueous solution by *Acer* tree leaves. The sorbent–sorbate equilibrium behavior is evaluated through fitting the experimental data to the major isotherm models. Additionally, the kinetics of the biosorption process is also investigated.

2. Materials and methods

2.1. Biosorbent materials

The *Acer* tree leaves were gathered from twigs into clean plastic bags washed with doubly distilled water and dried on a clean table at room temperature. The dried leaves were ground and sieved to the required particle size of about 0.074 mm, and then stored into plastic bags.

2.2. Batch procedure

All chemicals used were of analytical reagent grade (Merck, Darmstadt, Germany) and were used without further purification. A stock solution of MB (1,000 mg L^{-1}) was prepared in doubly distilled water. In a typical run, 10 mL of fresh MB solution was used, and a known amount of dried biomass was added to each sample solution. The pH of the solution was adjusted with HNO_3 or NaOH before adding the biosorbent. The mixture was shaken at 300 rpm (IKA-OS_2 Basic Orbital Shaker, Germany), at a known temperature, for 40 min. Filtration was performed using 0.45 mm Whatman filter paper.

2.3. Dye analysis

The concentration of the remaining MB in the solution after biosorption was determined using a UV–vis spectrophotometer (Analytikjena SPECORD250). Consequently, the following equations have been utilized for determining the removal percent (R) and amount of dye uptake per unit of adsorbent (q) from the aqueous solution:

$$q = \frac{(C_0 - C_e)V}{m} \tag{1}$$

$$R\ (\%) = \frac{(C_0 - C_e)}{C_0} \times 100 \tag{2}$$

where C_0 is the MB initial concentration (mg L^{-1}); C_e is the equilibrium dye concentration; V is the volume of solution (L); and m is the sorbent mass (g).

2.4. Fourier transform infrared spectroscopy

The Fourier transform infrared (FT-IR) spectra of MB and biomass were taken before and after MB loading in a range of 400–4,000 cm^{-1} using a Unicam-Galaxy series FT-IR 5000. In order to identify functional groups of *Acer* tree leaves and the possible interaction between functional groups and MB, 0.1 g of *Acer* tree leaf was loaded along with a 10 mL MB solution of 300 mg L^{-1} in 250 mL Erlenmeyer flasks and shaken at a rate of 300 rpm for 40 min at room temperature.

2.5. Hybrid design as optimization approach

In 1976, Roquemore developed a class of designs that are referred to as *hybrid designs* because the designs are related to central composite designs but are constructed to satisfy other criteria. There are multiple

designs for each number of factors. For example, for three factors, the designs were labeled 310, 311A, and 311B. Hybrid designs were created to achieve the same degree of orthogonality as central composite or regular polyhedral designs, to be at the near-minimum point, and to be near-rotatable. They resemble central composite designs which have been augmented with an extra variable column. Eight designs are presented, covering 3, 4, and 6 variables. All of these are at or within one point of the minimum [39]. During optimization, the relationship between the response, the main variables, and interactions were formulated as a quadratic model that includes the linear terms, thus:

$$Y = \beta_0 + \sum_{i=1}^{k} \beta_i x_i + \sum_{i=1}^{k} \beta_{ii} x_i^2 + \sum_{i=1}^{k-1} \sum_{j=2}^{k} \beta_{ij} x_i x_j + \varepsilon \qquad (3)$$

where y is the predicted response (MB biosorption capacity); β_0 is the offset term; β_i is the coefficient of linear effect; β_{ii} is the coefficient of squared effect; β_{ij} is the coefficient of interaction effect; and ε is the random error. They were estimated by multiple non-linear regression analysis. Surfaces were then built using the quadratic model for the statistically significant variables. The DESIGN EXPERT statistical software 8.0.7.1 was used for regression analysis of the obtained data and to estimate the coefficient of regression equation.

3. Results and discussion

3.1. Biosorbent characterization by FT-IR

A FT-IR spectrophotometer was used to better understand the nature of the functional groups responsible for MB binding. The FT-IR spectra of biosorbent and dye-loaded biosorbent are displayed in Fig. 1. The spectrum analysis of Fig. 1(A) shows that the broad peak at 3,369.85 cm^{-1} can be attributed to the O–H and N–H stretching vibrations. Due to C–H stretching vibrations of CH, CH_2, and CH_3 groups, the peaks at 2,920.41 and 2,850.97 cm^{-1} have been observed. The absorption band at 1,637.67 cm^{-1} is a characteristic of the carboxylate group. The intense peak at 1,072.49 cm^{-1} and the peak at 1,246.09 cm^{-1} are both due to C–O and C–N stretching vibrations. However, after absorbing of the MB onto the *Acer* tree leaf powder there are different changes in some peaks. The C=O stretching band exhibits a clear shift to a lower frequency at 1,620.30 cm^{-1}, while the C–O band increases to higher frequency at 1,039.70 cm^{-1}. It corresponds to the interaction of MB to C=O and C–O bands (Fig. 1(B)). The variation of intensity and shift of the band from 3,369.85 to 3,394.93, 1,637 to 1,620.31, and 1,072.49 to 1,039.70 cm^{-1} verifies that two functional groups, both carboxyl and either amine or hydroxyl (phenolic), are involved in MB binding [41,42].

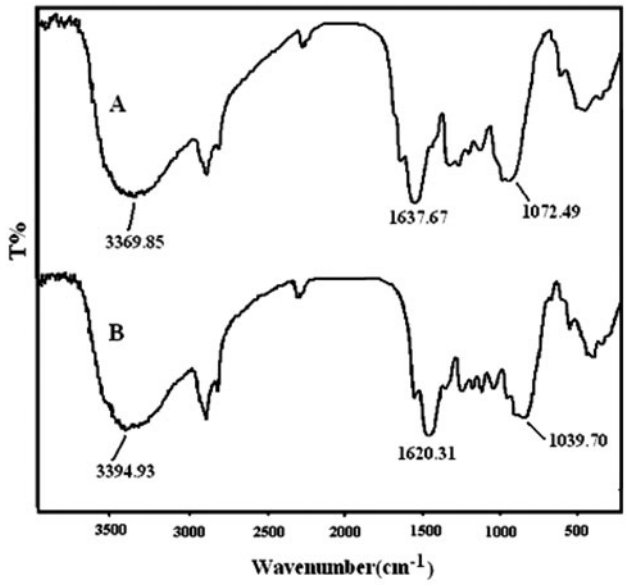

Fig. 1. FT-IR spectra of biosorbent (A) and MB loaded onto biosorbent (B).

3.2. Response surface as optimization approach

The RSM requires a mathematical model to be found capable of predicting the response. The optimized model was obtained through performing the hybrid central composite design. Three important factors, such as the initial concentration of MB in aqueous solutions C_0 (mg L^{-1}), the initial pH of the solution, and the sorbent mass (m) are considered as independent variables. Their experimental ranges and their levels for hybrid matrix design are shown in Table 1. The derived matrix design for running hybrid central composite design is shown in Table 2. By applying

Table 1
Experimental ranges and levels of effective variables

Coded values	MB (mg L^{-1})	pH	m
−1.41	50.63	2.04	0.02
−1.0000	–	3.2	0.05
−0.7071	338.06	–	–
0	625.5	6	0.11
0.7071	912.94	–	–
1	–	8.8	0.18
1.41	1,200.37	9.96	0.21

multiple regression analysis to the experimental data, the experimental results of the hybrid design are fitted with a full second-order polynomial equation. The empirical relationship between response (q) and effective variables obtained as coded values is given:

$$q = +35.60 - 5.11\,\mathrm{pH} - 6.56\,m + 14.16\,C + 6.16\,\mathrm{pH} \times m - 3.67\,\mathrm{pH} \times C - 2.34\,m \times C + 1.42\,\mathrm{pH} - 5.64\,C^2 \quad (4)$$

where q represents the predicted MB adsorption capacity of biosorption process. Analysis of variance (ANOVA) results for the model terms and regression coefficients of the suggested second-order equation are illustrated in Tables 3 and 4, respectively. Fisher's F test, resultant through the ANOVA, where the larger F-values and the smaller P-values indicate the more significant terms of the model, is run. The values of $p < 0.05$ also indicate significant regression at 95% confidence level. The "Lack of Fit p-value" of 0.250 implies that the lack of fit is not significantly relative to the pure error of experimental data of matrix design (Table 2). Goodness-of-fit for this model was also evaluated by the coefficient of determination. In this case, $R^2 = 0.999$ means that fit is very good and only 0.1% of total variance was not explained by the model. The high value of the adjusted coefficient of determination ($R^2_{adj} = 0.998$) is also an indication of the high significance of the proposed model. Furthermore, the model's adequacy has been investigated by examination of the residuals ($e = R_{exp} - R_{predic}$). The residual analysis outlines a good concordance between experimental and predicted responses. Further, the normal probability plot shows that the distribution of residuals is normal and the model satisfies the assumptions of the ANOVA [29–34]. The response surface plots are shown in Fig. 2(a)–(c), and clearly represent the effect of experimental variables and their mutual interactions on MB biosorption capacity. As the model explains, the sorbent mass has a negative effect, while concentration of MB has a positive consequence on adsorption capacity. As it can be observed from Fig. 2(a)–(c), the predicted model is visualized by the equation of q (Eq. (4)) as a function of two independent variables, while the third is being kept constant (at the middle point). Visual inspections of surfaces clearly show the interaction of effective variables, and the maximum MB biosorption capacity conditions which resulted ($q_{max} = 69.2\,mg\,g^{-1}$) at the initial concentration of MB 928 ($mg\,L^{-1}$), pH 2.7 and sorbent mass 0.05 g. These optimum conditions were also found through running DESIGN EXPERT software.

Table 2
Hybrid matrix design obtained and predicted response results

Standard order	C	m	pH	q_{exp}	q_{pred}
1	1,200.37	0.11	6.0	44.39	44.33
2	50.63	0.11	6.0	4.57	4.29
3	912.94	0.05	3.2	66.17	66.28
4	912.94	0.05	8.8	38.45	38.56
5	912.94	0.18	3.2	37.43	37.54
6	912.94	0.18	8.8	34.34	34.45
7	338.06	0.11	9.9	22.16	22.05
8	338.06	0.11	2.0	29.28	29.17
9	338.06	0.21	6.0	15.28	15.84
10	338.06	0.02	6.0	29.14	29.70
11	625.50	0.11	6.0	35.69	35.60
12	625.50	0.11	6.0	35.40	35.60
13	625.50	0.11	6.0	36.52	35.60
14	625.50	0.11	6.0	35.80	35.60

Table 3
ANOVA for the suggested second-order model

Source	DF[a]	SS[b]	MS[c]	F[d]	P[e]
Regression	8	2,580.64	322.58	942.22	<0.0001
Residual error	5	1.71	0.34		
Lack-of-fit	2	1.03	0.52	2.28	0.2,501
Pure error	3	0.68	0.23		
Total	13	2,582.35			

Notes:
[a]DF = Degree of freedom.
[b]SS = Sum squares.
[c]MS = Mean square (SS/DF).
[d]F = Fisher ratio.
[e]P = Significance level.

Table 4
Estimated effects and coefficients for the suggested second-order model

Predictor	Estimate	Coeff.	p
m	–248.4175	–6.56	<0.0001
C	+0.1070	14.16	<0.0001
pH	–5.8740	–5.11	<0.0001
pH × m	+33.8324	+6.16	<0.0001
pH × C	-3.2213×10^{-3}	–3.67	<0.0001
$C \times m$	–0.08864	–2.34	0.0005
pH^2	+0.1811	+1.42	0.0012
C^2	-3.4158×10^{-5}	–5.64	< 0.0001

Notes: $R^2 = 99.9\%$, R^2 (adj) = 99.83%.

3.3. Adsorption isotherms

The adsorption isotherms, through a description of sorbate–sorbent behavior, provide a quantitative

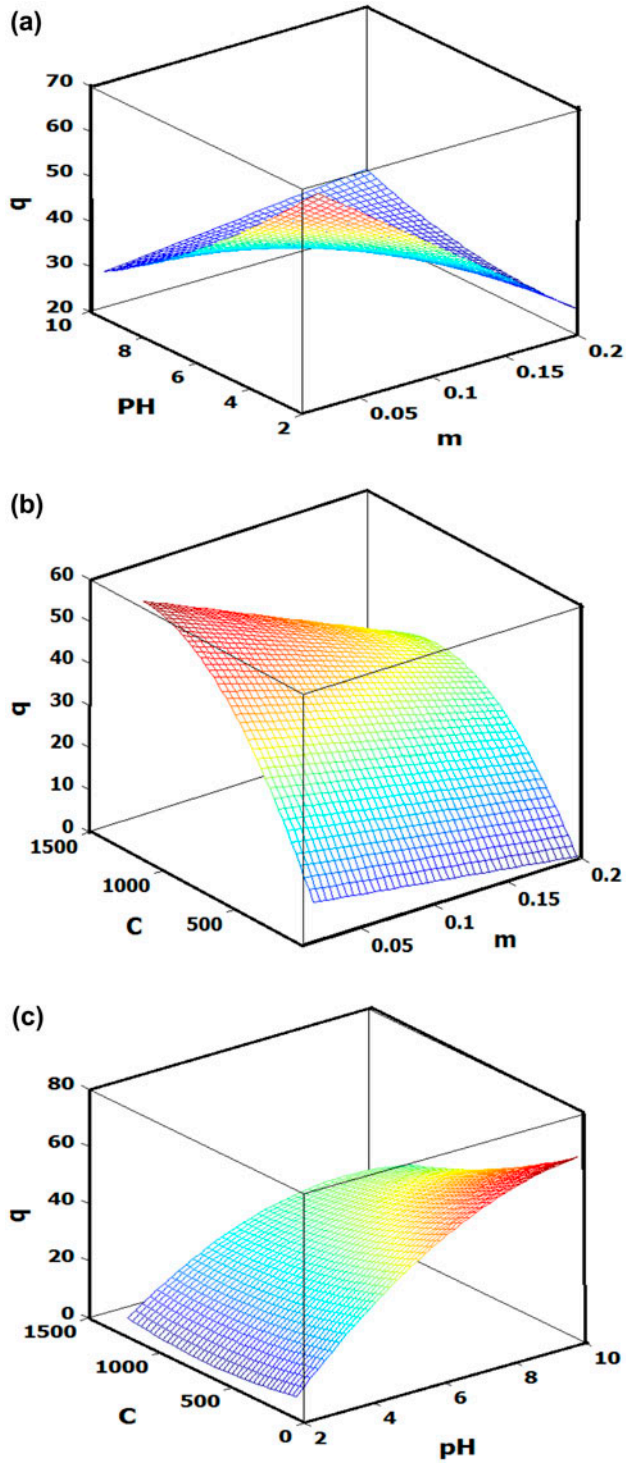

Fig. 2. Response surface plots showing; (a) the effects of biosorbent amount (*m*), pH and their mutual effect on the MB biosorption capacity, while the other variable is at the center level, (b) the effect of biosorbent amount (*m*), initial MB concentration, (*C*) and their mutual effect on the MB biosorption capacity, while the other variable is at the center level, (c) the effect of pH, initial MB concentration, (*C*) and their mutual effect on the MB biosorption capacity, while the other variable is at the center level.

estimation of adsorption capacity or maximum removal capacity of pollutant per unit mass of biosorbent; hence it is helpful in the planning of adsorption systems. In this study, the experimental data are fitted to Langmuir, Freundlich, and Dubinin–Radushkevich (D–R) isotherm equations (Fig. 3) [43–51]. The Langmuir model suggests that pollutant removal from the aqueous phase occurs on homogeneous surfaces by monolayer sorption without interactions between sorbate molecules, and the adsorption of each molecule onto the surface has equal adsorption activation energy. Conversely, the Freundlich isotherm assumes a heterogeneous surface with a non-uniform distribution for heat of adsorption over the surface and a multilayer adsorption can be expressed. The Langmuir and Freundlich isotherms are represented by the following equations, respectively:

Langmuir:

$$q_e = \frac{q_{\max} b C_e}{1 + b C_e} \tag{5}$$

Freundlich:

$$q_e = K_F C_e^{\frac{1}{n}} \tag{6}$$

where $q_{\max}$ is the maximum amount of adsorption (mg g^{-1}); q_e is the adsorption capacity at equilibrium (mg g^{-1}); b is the adsorption equilibrium constant

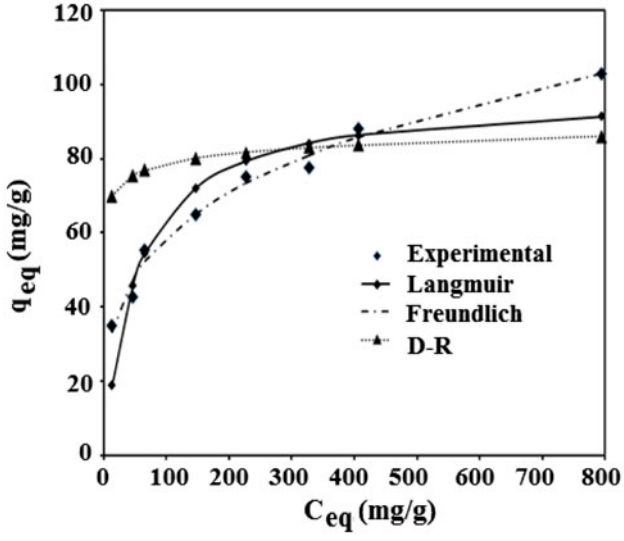

Fig. 3. Non-linear fits of Langmuir, Freundlich, and D–R isotherm models for MB onto *Acer* tree leaves ($T = 25$ ℃; pH 2.7 ; $m = 0.05$ g).

($L\,mg^{-1}$); C_e is the equilibrium concentration of sorbate in the solution ($mg\,L^{-1}$); K_F is the constant ($mg\,g^{-1}$) representing the adsorption capacity; and n is the constant depicting the adsorption intensity. Thus, the experimental equilibrium data were fitted to both Langmuir and Freundlich isotherms and obtained results are presented at Table 5. In order to predict the biosorption mechanism the equilibrium data were also examined with the D–R isotherm model (isotherm). It is applied to distinguish between the physical and chemical biosorptions of MB. The D–R model describes the biosorption nature of the sorbate on biosorbent, and it is utilized to calculate the mean free energy of biosorption. The D–R equation is generally expressed as follows [47–51]:

$$q_e = q_m \exp(-\beta\varepsilon^2) \tag{7}$$

where $\varepsilon = RT\ \ln(1 + 1/C_e)$ (Polanyi potential); q_e is the amount of MB biosorbed per unit weight of biosorbent at equilibrium ($mg\,g^{-1}$); q_m is the maximum biosorption capacity ($mg\,g^{-1}$); C_e is the equilibrium concentration of MB in aqueous solution ($mg\,L^{-1}$); β is the constant related to the biosorption energy; R is the gas constant; and T is the absolute temperature (K). The mean free energy of biosorption (E) is defined as free-energy change when one mol of MB has been transferred from infinity in solution to the surface of the solid. This parameter can be calculated from the β value obtained from the above equation.

Table 5
Constant parameters and different criteria calculated for non-linear fitting of various adsorption isotherms

Isotherm	Parameters	Value
Freundlich	K_f ($mg\,g^{-1}$)	16.86
	n	3.69
	R^2	0.9986
	Δq	0.046
	χ^2	1.01
Langmuir	q_{max} ($mg\,g^{-1}$)	97.07
	b ($L\,mg^{-1}$)	0.0196
	R^2	0.9872
	Δq	0.159
	χ^2	17.0
Dubinin–Redushkevich (D–R)	q_{max} ($mg\,g^{-1}$)	95.85
	B $(mol^2\,(kJ)^2)^{-1}$	5×10^{-10}
	E ($kJ\,mol^{-1}$)	31.6
	R^2	0.9242
	Δq	0.428
	χ^2	44.95

$$E = \frac{1}{\sqrt{-2\beta}} \tag{8}$$

From the magnitude of E, the types of biosorption, such as chemisorption or physical sorption can be determined. If $E = 8$–$16\ kJ\,mol^{-1}$, then chemical ion-exchange dominates the reaction. If $E < 8\ kJ\,mol^{-1}$, then physical biosorption takes place, while chemisorption processes have adsorption energy in the range of 20–$40\ kJ\,mol^{-1}$ [30,33,34,46–51]. The mean free energy of biosorption (E) is found to be $31.6\ kJ\,mol^{-1}$. It implies that biosorption of MB on *Acer* tree leaves is chemical adsorption. To quantitatively compare the applicability of each model, an error function is required. As a result, normalized standard deviation (Δq), the coefficient of determination (R^2), and Chi-square (χ^2) statistics are calculated as follows [44,46]:

$$R^2 = \sum \left(q_{e,\exp} - \bar{q}_{\text{calc}}\right)^2 / \sum \left(\left(q_{e,\exp} - \bar{q}_{\text{calc}}\right)^2 + \left(q_{e,\exp} - \bar{q}_{\text{calc}}\right)^2\right) \tag{9}$$

$$\Delta q = \sqrt{\frac{\sum \left[\left(q_{e,\exp} - q_{e,\text{cal}}\right)/q_{e,\exp}\right]^2}{n-1}} \tag{10}$$

$$\chi^2 = \sum \frac{\left(q_{e,\exp} - q_{e,\text{cal}}\right)^2}{q_{e,\text{cal}}} \tag{11}$$

where n is the number of data points and q_e is sorbent capacity at the equilibrium experimental condition ($q_{e,\exp}$) and calculated ($q_{e,\text{cal}}$), respectively. These criteria provide a numerical estimate to measure the goodness of fit of a given mathematical model to the data, their plot being shown in Fig. 3. The parameters of isotherm models listed in Table 5 are determined by means of a non-linear regression method. The comparison of these criteria for studied isotherms leads to a different conclusion. If R^2 is chosen, the order of goodness of fit for considered isotherms are: Freundlich ($R^2 = 99.86$) > Langmuir ($R^2 = 98.72$) > D–R ($R^2 = 92.42$). However, judgment according to Δq and χ^2 leads to the same order such as: Freundlich ($\Delta q = 0.046$, $\chi^2 = 1.01$) > Langmuir ($\Delta q = 0.159$, $\chi^2 = 17.0$) > (D–R) ($\Delta q = 0.428$, $\chi^2 = 44.96$). The higher coefficient of determination also indicates that both the Langmuir and Freundlich models were suitable for describing the adsorption equilibrium of MB by the adsorbent, but the equilibrium data fitted better to the Freundlich isotherm as compared to Langmuir model in the concentration ranges studied. The applicability of both models implies that monolayer adsorption, as well as

heterogeneous surface conditions, may co-exist under the adjusted experimental conditions. On average, a favorable adsorption tends to have Freundlich constant n between 1 and 10. Larger values of n (smaller value of $1/n$) imply stronger interaction between adsorbent and dye, while $1/n$ equal to one, indicates linear adsorption leading to identical adsorption energies for all sites.

3.4. Adsorption kinetics

To understand the mechanism of the biosorption process, kinetic study is a helpful approach. Kinetic studies of adsorption for MB onto an *Acer* tree leaf were carried out at the initial concentration of 100.0 mg L^{-1} (in 150 mL flask during shaking at 300 rpm) for contact times in the range of 2–90 min. As depicted in Fig. 4(a), the adsorption of MB is rapid and an interaction period of 15 min supplies about 70% adsorption. Such effective dye elimination in a short period of time would be privileged over other low-cost adsorbents when exploiting industrial wastewater. To understand the mechanism of the biosorption process and determine the rate of the dominating step, the biosorption data were analyzed using the three simplest kinetic models: pseudo-first-order, pseudo-second-order, and intra-particle diffusion [45–51]. The best-fitted model was chosen according to the linear regression coefficient of determination, R^2 values. The Lagergren equation that can be given as the following expression suggests the pseudo-first-order rate.

$$\ln (q_e - q_t) = \ln q_e - K_1 t \tag{12}$$

where q_e and q_t are the MBs biosorbed at equilibrium and time t (mg g^{-1}), respectively. K_1 is the rate constant for pseudo-first-order biosorption (min^{-1}). The low value of coefficient of determination ($R^2 = 0.49$) shows that biosorption of MB onto *Acer* tree leaves does not follow the pseudo-first-order kinetic.

The biosorption kinetic can also be evaluated by a pseudo-second-order rate model (Eq. (13)), and the model plots are given in Fig. 4(b).

$$\frac{t}{q_t} = \frac{1}{k_2 q_2^2} + \frac{1}{q_2} t \tag{13}$$

where q_2 is the maximum biosorption capacity (mg g^{-1}) for the pseudo-second-order biosorption; q_t is the amount of MB biosorbed at time t (mg g^{-1}); and k_2 is the equilibrium rate constant of pseudo-second-order biosorption (g mg^{-1} min). Values of k_2 and q_2 were calculated to be 0.0,264 (g mg^{-1} min) and 16.39 (mg g^{-1}), respectively from the plot of t/q against t. The coefficient of determination for the second-order kinetics model (R^2) is greater than 0.999, which indicates the better applicability of this kinetic equation and the second-order nature of the adsorption process

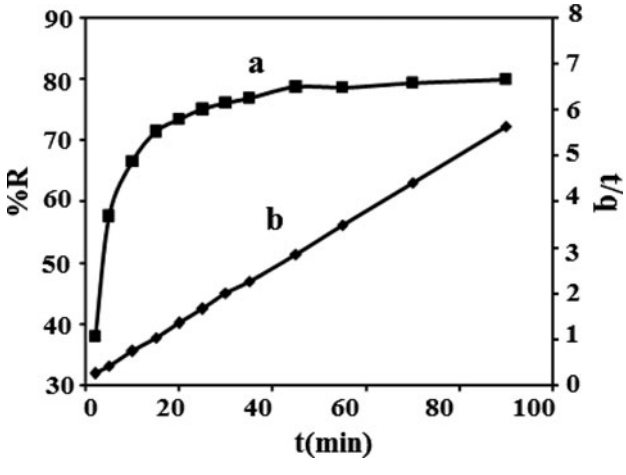

Fig. 4. (a) Effect of contact time on MB-removal efficiency ($T = 25$ °C, $m = 0.05$ g, pH 6, initial conc. of MB = 100 mg L^{-1}) and (b) Pseudo-second-order kinetic plot for the sorption of MB onto *Acer* tree leaves.

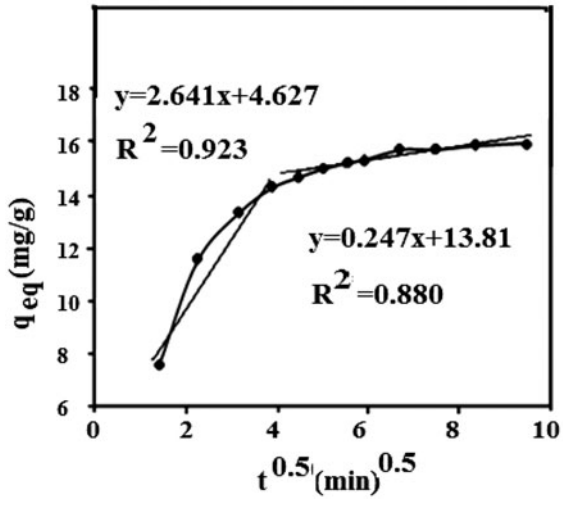

Fig. 5. Intra-particle diffusion plot for the adsorption of MB onto *Acer* tree leaves efficiency ($T = 25$ °C, $m = 0.05$ g, pH 6, initial conc. of MB = 100 mg L^{-1}).

Table 6
Comparisons of biosorption of MB with different biosorbents

Biosorbent	Q_{max} mg g^{-1}	Reference
Citrus sinensis bagasse	96.40	[27]
Algal waste	104	[52]
Dead fungus *Aspergillus niger*	18.54	[53]
Green alga *Ulva lactuca*	40.2	[54]
Chemically treated guava leaves	133.33	[55]
Saw dust	133.87	[56]
Dehydrated peanut hull	108.6	[57]
Teak wood bark	84	[58]
Yellow passion fruit waste	44.7	[59]
Hazelnut shell	38.22	[60]
Salsola vermiculata leaves	23	[61]
Banana peel	20.8	[62]
Orange peel	18.6	[62]
Wheat shells	16.56	[63]
Neem (*Azadirachta indica*) leaf powder	3.67	[64]
Acer tree leaves	97.07	This work

of MB onto *Acer* tree leaves. Weber's intra-particle diffusion model was further employed to identify the steps involved during the biosorption process, which is described as:

$$q_t = k_i t^{\frac{1}{2}} + C \quad (14)$$

where q_t is the uptake at any time (mg g^{-1}); k_i is the intra-particle diffusion constant (mg min$^{0.5}$ g^{-1}); and C is the intercept. According to the Morris and Weber theory, a plot of q_t vs. $t^{1/2}$ should be linear if intra-particle diffusion is involved in the adsorption process, and if this line passes through the origin, then intra-particle diffusion is the rate-controlling step [45–51].

As it can be seen from Fig. 5, the intra-particle diffusion ($C = 4.627$, $R^2 = 0.923$) is not the only rate-determining step in the biosorption kinetic process of MB on *Acer* tree leaves. The calculated value of the intra-particle diffusion constant (k_i) was 2.641 mg min$^{0.5}$ g^{-1}. According to Fig. 5, the plot presents multi-linearity, thus indicating that two or more steps take place. The initial region is a diffusion adsorption stage, attributed to the diffusion of dye through the solution to the external surface of the adsorbent (external diffusion). The second region is a gradual adsorption stage, corresponding to intra-particle diffusion of dye molecules through the pores of adsorbent (intra-particle diffusion). Therefore, both film diffusion and intra-particle diffusion processes are simultaneously operating MB adsorption onto the biosorbent. The observed multi-linearity also suggests that intra-particle diffusion is not the rate-limiting step.

Comparison of biosorption of MB by some biosorbents is shown in Table 6. As can be seen, *Acer* tree leaves have a significant potential for adsorption of MB from an aqueous solution [27].

4. Conclusion

The aim of this work was to find the possible use of *Acer* tree leaves as an effective biosorbent for the removal of MB from aqueous solutions. Hybrid central composite design was applied to find a suitable model that would lead to optimum outcome conditions. The optimum biosorption conditions were determined as initial concentration MB 928 mg L^{-1}, pH 2.7 and sorbent mass 0.05 g. Consequently, the maximum MB biosorption capacity resulted ($q_{max} = 69.2$). Obtained results were fitted to different isotherm equations. The Freundlich isotherm model matched better with the equilibrium data, since it presents higher R^2 values than with others. In kinetic study, the pseudo-second-order kinetic model was found to be well suited for the entire adsorption process of MB on a biosorbent.

References

[1] E. Forgacs, T. Cserháti, G. Oros, Removal of synthetic dyes from wastewaters: A review, Environ. Int. 30 (2004) 953–971.
[2] M. Rafatullah, O. Sulaiman, R. Hashim, A. Ahmad, Adsorption of methylene blue on low-cost adsorbents: A review, J. Hazard. Mater. 177 (2010) 70–80.
[3] M.R. Sohrabi, M. Ghavami, Photocatalytic degradation of direct red 23 dye using UV/TiO_2: Effect of operational parameters, J. Hazard. Mater. 153 (2008) 1235–1239.

[4] M. Sleiman, D.L. Vildozo, C. Ferronato, J.M. Chovelon, Photocatalytic degradation of azo dye metanil yellow: Optimization and kinetic modeling using a chemometric approach, Appl. Catal. B 77 (2007) 1–11.
[5] M. Abbasi, N.R. Asl, Sonochemical degradation of basic blue 41 dye assisted by nanoTiO_2 and H_2O_2, J. Hazard. Mater. 153 (2008) 942–947.
[6] N. Zaghbani, A. Hafiane, M. Dhahbi, Removal of safranin T from wastewater using micellar enhanced ultrafiltration, Desalination 222 (2008) 348–356.
[7] J.S. Wu, C.H. Liu, K.H. Chu, S.Y. Suen, Removal of cationic dye methyl violet 2B from water by cation exchange membranes, J. Membr. Sci. 309 (2008) 239–245.
[8] L. Fan, Y. Zhou, W. Yang, G. Chen, F. Yang, Electrochemical degradation of aqueous solution of amaranth azo dye on ACF under potentiostatic model, Dyes Pigm. 76 (2008) 440–446.
[9] M.X. Zhu, L. Lee, H.H. Wang, Z. Wang, Removal of an anionic dye by adsorption/precipitation processes using alkaline white mud, J. Hazard. Mater. 149 (2007) 735–741.
[10] G. Sudarjanto, B. Keller-Lehmann, J. Keller, Optimization of integrated chemical–biological degradation of a reactive azo dye using response surface methodology, J. Hazard. Mater. 138 (2006) 160–168.
[11] V. Sarria, M. Deront, P. Peringer, C. Pulgarin, Degradation of a biorecalcitrant dye precursor present in industrial wastewaters by a new integrated iron(III) photoassisted-biological treatment, Appl. Catal. 40 (2003) 231–246.
[12] J. García-Montaño, L. Pérez-Estrada, I. Oller, M.I. Maldonado, F. Torrades, J. Peral, Pilot plant scale reactive dyes degradation by solar photo-Fenton and biological processes, J. Photochem. Photobiol. A 195 (2008) 205–214.
[13] B. Lodha, S. Chaudhari, Optimization of Fenton-biological treatment scheme for the treatment of aqueous dye solutions, J. Hazard. Mater. 148 (2007) 459–466.
[14] B.H. Hameed, F.B.M. Daud, Adsorption studies of basic dye on activated carbon derived from agricultural waste: *Hevea brasiliensis* seed coat, Chem. Eng. J. 139 (2008) 48–55.
[15] F.C. Wu, R.L. Tseng, High adsorption capacity NaOH-activated carbon for dye removal from aqueous solution, J. Hazard. Mater. 152 (2008) 1256–1267.
[16] S.A. Saad, K.Md. Isaa, R. Bahari, Chemically modified sugarcane bagasse as a potentially low-cost biosorbent for dye removal, Desalination 264 (2010) 123–128.
[17] P. Janoš, S. Coskun, V. Pilařová, J. Rejnek, Removal of basic (methylene blue) and acid (egacid orange) dyes from waters by sorption on chemically treated wood shavings, Bioresour. Technol. 100 (2009) 1450–1453.
[18] R. Gong, M. Li, C. Yang, Y. Sun, J. Chen, Removal of cationic dyes from aqueous solution by adsorption on peanut hull, J. Hazard. Mater. 121 (2005) 247–250.
[19] A.N. Fernandes, C.A.P. Almeida, C.T.B. Menezes, N.A. Debacher, M.M.D. Sierra, Removal of methylene blue from aqueous solution by peat, J. Hazard. Mater. 144 (2007) 412–419.
[20] V.S. Mane, P.V.V. Babu, Studies on the adsorption of brilliant green dye from aqueous solution onto low-cost NaOH treated saw dust, Desalination 273 (2011) 321–329.
[21] F.A. Pavan, Removal of methylene blue dye from aqueous solutions by adsorption using yellow passion fruit peel as adsorbent, Bioresour. Technol. 99 (2008) 3162–3165.
[22] V. Ponnusami, V. Gunasekar, S.N. Srivastava, Kinetics of methylene blue removal from aqueous solution using gulmohar (*Delonix regia*) plant leaf powder: Multivariate regression analysis, J. Hazard. Mater. 169 (2009) 119–127.
[23] V. Ponnusami, K.S. Rajan, S.N. Srivastava, Application of film-pore diffusion model for methylene blue adsorption onto plant leaf powders, Chem. Eng. J. 163 (2010) 236–242.
[24] J. Zolgharnein, Zh. Adhami, A. Shahmoradi, S.N. Mousavi, Optimization of removal of methylene blue by *Platanus* tree leaves using response surface methodology, Anal. Sci. 26 (2010) 111–116.
[25] M.-C. Shih, Kinetics of the batch adsorption of methylene blue from aqueous solutions onto rice husk: Effect of acid-modified process and dye concentration, Desalin. Water Treat. 37 (2012) 200–214.
[26] V.M. Vučurović, R.N. Razmovski, N.M. Tekić, Methylene blue (cationic dye) adsorption onto sugar beet pulp: Equilibrium isotherm and kinetic studies, J. Taiwan Inst. Chem. Eng. 43 (2012) 108–111.
[27] H.N. Bhatti, N. Akhtar, N. Saleem, Adsorptive removal of methylene blue by low-cost citrus sinensis bagasse: Equilibrium, kinetic and thermodynamic characterization, Arab. J. Sci. Eng. 37 (2012) 9–18.
[28] S. Chatterjee, A. Kumar, S. Basu, S. Dutta, Application of response surface methodology for methylene blue dye removal from aqueous solution using low cost adsorbent, Chem. Eng. J. 181–182 (2012) 289–299.
[29] J. Zolgharnein, A. Shahmoradi, J.B. Ghasemi, Comparative study of Box–Behnken, central composite, and Doehlert matrix for multivariate optimization of Pb (II) adsorption onto Robinia tree leaves, J. Chemom. 27 (2013) 12–20.
[30] J. Zolgharnein, N. Asanjarani, S.N. Mousavi, Optimization and characterization of Tl(I) adsorption onto modified *Ulmus carpinifolia* tree leaves, Clean—Soil Air Water 39(3) (2011) 250–258.
[31] J. Zolgharnein, Zh. Adhami, A. Shahmoradi, S.N. Mousavi, M.R. Sangi, Multivariate optimization of Cd(II) biosorption onto *Ulmus* tree leaves from aqueous wastes, Toxicol. Environ. Chem. 92(8) (2010) 1461–1470.
[32] J. Zolgharnein, A. Shahmoradi, M.R. Sangi, Optimization of Pb(II) biosorption by *Robinia* tree leaves using statistical design of experiments, Talanta 76 (2008) 528–532.
[33] J. Zolgharnein, A. Shahmoradi, Adsorption of Cr(VI) onto *Elaeagnus* tree leaves; statistical optimization, equilibrium modeling and kinetic studies, J. Chem. Eng. Data 55 (2010) 3428–3437.
[34] J. Zolgharnein, A. Shahmoradi, Characterization of sorption isotherms, kinetic models, and multivariate approach for optimization of Hg(II) adsorption onto *Fraxinus* tree leaves, J. Chem. Eng. Data 55 (2010) 5040–5049.
[35] M.A. Bezerra, R.E.E. Santelli, P. Oliveira, L.S. Villar, L.A. Escaleira, Response surface methodology (RSM) as a tool for optimization in analytical chemistry, Talanta 76 (2008) 965–977.

[36] D.L. Massart, B.G.M. Vandeginste, L.M.C. Buydens, S. De Jong, P.J. Lewi, J. Smeyers-Verbeke, Handbook of Chemometrics and Qualimetrics, Part A, Elsevier, Amsterdam, 1997.
[37] R.E. Bruns, I.S. Scarmino, B. de Barros Neto, Statistical Design—Chemometrics, 1st ed., Elsevier, Amsterdam, 2006.
[38] D.C. Montgomery, Design and Analysis of Experiments, 5th ed., Wiley, New York, NY, 2001.
[39] T.P. Ryan, Modern Experimental Design, John Wiley, Hoboken, NJ, 2007.
[40] K.G. Roquemore, Hybrid designs for quadratic response surfaces, Technometrics 18 (1976) 419–423.
[41] K. Gobi, M.D. Mashitah, V.M. Vadivelu, Adsorptive removal of methylene blue using novel adsorbent from palm oil mill effluent waste activated sludge: Equilibrium, thermodynamics and kinetic studies, Chem. Eng. J. 171 (2011) 1246–1252.
[42] H. Chen, J. Zhao, G. Dai, Silkworm exuviae—A new non-conventional and low-cost adsorbent for removal of methylene blue from aqueous solutions, J. Hazard. Mater. 186 (2011) 1320–1327.
[43] Y. Liu, Y.J. Liu, Biosorption isotherms, kinetics and thermodynamics, Sep. Purif. Technol. 61 (2008) 229–242.
[44] K.Y. Foo, B.H. Hameed, Insights into the modeling of adsorption isotherm systems, Chem. Eng. J. 156 (2010) 2–10.
[45] L. Ai, C. Zhang, F. Liao, Y. Wang, M. Li, L. Meng, J. Jiang, Removal of methylene blue from aqueous solution with magnetite loaded multi-wall carbon nanotube: Kinetic, isotherm and mechanism analysis, J. Hazard. Mater. 198 (2011) 282–290.
[46] J. Zolgharnein, T. Shariatmanesh, N. Asanjarani, A. Zolanvari, Doehlert design as optimization approach for the removal of Pb(II) from aqueous solution by *Catalpa Speciosa* tree leaves: Adsorption characterization, Desalin. Water Treat. (in press). doi: 10.1080/19443994.2013.853625.
[47] S. Sadaf, H.N. Bhatti, Batch and fixed bed column studies for the removal of Indosol Yellow BG dye by peanut husk, J. Taiwan Inst. Chem. Eng. 45(2) (2014) 541–553.
[48] J. Mittal, V. Thakur, A. Mittal, Batch removal of hazardous azo dye Bismark Brown R using waste material *hen feather*, Ecol. Eng. 60 (2013) 249–253.
[49] S. Noreen, H.N. Bhatti, S. Nausheen, S. Sadaf, M. Ashfaq, Batch and fixed bed adsorption study for the removal of Drimarine Black CL-B dye from aqueous solution using a *lignocellulosic* waste: A cost affective adsorbent, Ind. Crop Prod. 50 (2013) 568–579.
[50] V.K. Gupta, A. Mittal, D. Jhare, J. Mittal, Batch and bulk removal of hazardous colouring agent Rose Bengal by adsorption techniques using bottom ash as adsorbent, RSC Adv. 2 (2012) 8381–8389.
[51] A. Mittal, D. Jhare, J. Mittal, Adsorption of hazardous dye eosin yellow from aqueous solution onto waste material De-oiled Soya: Isotherm, kinetics and bulk removal, J. Mol. Liq. 179 (2013) 133–140.
[52] V.J.P. Vilar, C.M.S. Botelho, R.A.R. Boaventura, Methylene blue adsorption by *algal biomass* based materials: Biosorbents characterization and process behaviour, J. Hazard. Mater. 147 (2007) 120–132.
[53] Y. Fu, T. Viraraghavan, Removal of a dye from an aqueous solution by the *fungus Aspergillus niger*, Water Qual. Res. J. Can. 5(1) (2000) 95–111.
[54] A. El Sikaily, A. Khaled, A. Nemr, O. Abdelwahab, Removal of methylene blue from aqueous solution by marine green alga *Ulva lactuca*, Chem. Ecol. 22(2) (2006) 149–157.
[55] D.K. Singh, B. Srivastava, Removal of basic dyes from aqueous solutions by chemically treated *Psidium guyava leaves*, Indian J. Environ. Health 41 (1999) 333–345.
[56] S. Chakraborty, S. De, S. Dasgupta, J.K. Basu, Removal of dyes from aqueous solution using a low cost adsorbent, in: Water and Wastewater Perspectives of Developing Countries, Proceedings of International Conference, International Water Association, New Delhi, 2002, pp. 1089–1096.
[57] D. Ozer, G. Dursun, A. Ozer, Methylene blue adsorption from aqueous solution by dehydrated peanut hull, J. Hazard. Mater. 144 (2007) 71–179.
[58] G. McKay, G. Ramprasad, P. Pratapa Mowli, Equilibrium studies for the adsorption of dyestuffs from aqueous solutions by low-cost materials, Water Air Soil Pollut. 29 (1986) 273–283.
[59] F.A. Pavan, E.C. Lima, S.L.P. Dias, A.C. Mazzocato, Methylene blue biosorption from aqueous solutions by yellow passion fruit waste, J. Hazard. Mater. 150 (2008) 703–712.
[60] M. Doğan, H. Abak, M. Alkan, Biosorption of methylene blue from aqueous solutions by hazelnut shells: Equilibrium, parameters and isotherms, Water Air Soil Pollut. 192 (2008) 141–153.
[61] B. Bestani, N. Benderdouche, B. Benstaali, M. Belhakem, A. Addou, Methylene blue and iodine adsorption onto an activated *desert plant*, Bioresour. Technol. 99 (2008) 8441–8444.
[62] G. Annadurai, R. Juang, D. Lee, Use of cellulose-based wastes for adsorption of dyes from aqueous solutions, J. Hazard. Mater. 92 (2002) 263–274.
[63] Y. Bulut, H.A. Aydin, A kinetics and thermodynamics study of methylene blue adsorption on wheat shells, Desalination 194 (2006) 259–267.
[64] K.G. Bhattacharyya, A. Sharma, Kinetics and thermodynamics of methylene blue adsorption on Neem (*Azadirachta indica*) leaf powder, Dyes Pigm. 65 (2005) 51–59.